Supporting Information

Alkyne-Functionalized Superstable Graphitic Silver Nanoparticles for Raman Imaging

Zhi-Ling Song,[†] Zhuo Chen,[*†] Xia Bian,[†] Li-Yi Zhou,[†] Ding Ding,[†] Hao Liang,[†] Yu-Xiu Zou,[†] Shan-Shan Wang,[†] Long Chen,[§] Chao Yang,[†] Xiao-Bing Zhang*[†] and Weihong Tan[*†‡]

Email: zhuochen@hnu.edu.cn, xbzhang@hnu.edu.cn, tan@chem.ufl.edu

[†]Molecular Sciences and Biomedicine Laboratory, State Key Laboratory for Chemo/Biosensing and Chemometrics, College of Chemistry and Chemical Engineering, College of Biology, Collaborative Innovation Center for Molecular Engineering and Theronastics, Hunan University, Changsha 410082, China

[‡]Department of Chemistry and Department of Physiology and Functional Genomics, Center for Research at Bio/nano Interface, Shands Cancer Center, UF Genetics Institute and McKnight Brain Institute, University of Florida, Gainesville, Florida 32611-7200, United States

[§]Faculty of Sciences University of Macau, Av. Padre Tomás Pereira Taipa, Macau, China

Table of Contents

1. Supplemental Materials and Methods

Reagents. Anhydrous silver nitrate ($AgNO_3$), hydrous copper nitrate ($CuNO_3 \cdot 3H_2O$) and R6G (Rhodamine 6G) were obtained from Aladdin. Polyoxyethylenestearyl ether was purchased from Sigma Aldrich. 4-Iodobenzyl alcohol and phenylacetylene were obtained from J&K Chemical. Dichloromethane (DCM), phosphorus tribromide (PBr_3), triphenyl phosphine (PPh_3), bis (triphenylphosphine) palladium(II) chloride ($PdCl_2(PPh_3)_2$), hexane, cuprous iodide (CuI), ethyl acetate (EtOAc), and tetrahydrofuran (THF) were obtained from Changsha Chemical Reagents Company (Changsha, China). All other chemicals of analytical reagent grade were obtained from Changsha Chemical Reagents Company (Changsha, China) and used as received without further purification. Doubly distilled water (resistance > 18 M Ω cm^{-1}) was used throughout all experiments.

Synthesis of ACGs. ACGs were produced in a chemical vapor deposition (CVD) system. First, fumed silica (1.50 g, Aladdin) was impregnated with $AgNO_3$ (365 mg) and $CuNO_3 \cdot 3H_2O$ (131 mg) in methanol and sonicated for 2 h. The mixture was then dried at 80 °C, and the powder was ground. Typically, 0.50 g of the powder was used for methane CVD in a tube furnace. The sample grew with a methane flow of 250 $cm^3\ min^{-1}$ for 15 minutes. After growth, the sample was etched with HF and HNO_3 to dissolve the silica and the uncovered AgCu particles. The ACG solid product was then washed thoroughly and collected through centrifugation. To further investigate the influence of Ag/Cu ratio to plasmonic properties, ACGs with two different Ag/Cu ratios were prepared and characterized by the Optima 8000 ICP-MS (PerkinElmer, Table S1), as well as the UV-2450 UV-vis spectrophotometer (Shimadzu, Figure S2). Increasing the Ag/Cu ratio in the ACGs leads to the relatively higher LSPR peak around 400 nm.

Synthesis of (4-phenylethynyl)-benzylamino polyethylene glycol (alkyne-PEG). (4-phenylethynyl) benzyl alcohol was first synthesized. 4-iodobenzyl alcohol (4.3 mmol), PPh_3 (0.085 mmol) and CuI (0.085 mmol) were dissolved in solution, including 10 mL dried THF and 5 mL dried triethylamine. After degassing, $PdCl_2(PPh_3)_2$ (0.026 mmol) was added to the solution. The mixture was degassed again, and phenylacetylene (4.3 mmol) dissolved in 2 mL dried THF was added dropwise. The mixture was stirred at 50 °C overnight in nitrogen atmosphere. 50 mL of iced water were added to the solution, followed by drying with $MgSO_4$. The solvent was removed under reduced pressure, and the pure product was gained in 99% isolated yield. While maintaing the temperature at 0°C, phosphorus tribromide was added to 5ml DCM solution containing (4-Phenylethynyl)benzyl alcohol (1.44 mmol). After stirring 2 hours at 0 °C, the solvent was removed under reduced pressure. The (4-Phenylethynyl)benzyl bromide product was purified by flash chromatography[1] (Petroleum ether/EtOAc, 50:50) to get the compound in 100 % isolated yield. MS (EI) calcd for $C_{15}H_{12}Br$ m/z 270.0, found 270.1 (M+). Then (4-Phenylethynyl) benzyl

bromide (0.3 mmol) and NH_2-PEG (MW=1000, 0.15 mmol) were dissolved in acetone in the presence of K_2CO_3.[2] The mixture was stirred 12 h at room temperature to obtain the alkyne-PEG.

Surface functionalization of ACG. ACG powder was added to the polyoxyethylenestearyl ether aqueous solution and sonicated for 1 hour. The soluble ACG was washed three times through centrifugation to remove the free polyoxyethylenestearyl ether. For alkyne-PEG functionalization of ACG, alkyne-PEG was dissolved in water and acetone (volume 2:1); then, ACG power and polyoxyethylenestearyl ether was added to the solution and sonicated for 1hour. The mixture was washed 4 times with water through centrifugation to remove the free alkyne-PEG.

Cell culture. Human breast cancer cells (MCF-7) were cultured at 37 °C in RPMI 1640 medium supplemented with 10% premium fetal bovine serum (FBS) and 1% penicillin-streptomycin in a 5% CO_2 environment.

Characterization of ACGs with transmission electron microscopy. Transmission electron microscopy (TEM, JEM-2010, Jeol, Japan) was applied to characterize the morphology and size distribution of ACGs. A crystalline face-centered-cubic AgCu core for the ACG was identified by selected area electron diffraction (SAED). Scanning transmission electron microscopy (STEM) imaging of ACG was performed by field emission electron microscopy (Tecnai G2F20 S-TWIN). Transmission electron microscopy (TEM), including more nanoparticles and hollow graphitic shell from etching the AgCu core, energy dispersive spectrometey (EDS) and selected area electron diffraction characterization were demonstrated in Figure S1, which confirmed the core-shell structure with an AgCu core and an AGC graphitic shell.

Stability tests of the ACGs aqueous solution. To further investigate the stability of the ACGs, different concentrations of H_2O_2 were utilized. Figure S3 showed the temporal changes of bare AgNPs and ACGs aqueous solution after adding 10 and 55 mM H_2O_2, respectively. The absorption peak of bare AgNPs decreased quickly within 20 minutes, and degradation was faster with the increase of concentration. In contrast, the absorption peaks around 400 nm and 600 nm of ACGs both showed few changes. Digital photos of bare AgNPs and ACGs added to H_2O_2 solution after different times were also shown in Figure S3. Bare AgNPs solution produced bubbles and became colorless because of the violent reaction of Ag and H_2O_2. As concentration increased, oxidation occurred more rapidly. However, no obvious changes were observed in the ACGs aqueous solution. The corrosion-resistant capabilites of ACGs to NaHS (Figure S4) and HNO_3 (Figure S5) were also investigated. ACGs all demonstrated superior stability over that of the bare AgNPs, further confirming successful encapsulation of the graphitic shells.

Stability tests of the AgCu NPs. For comparison, bare AgCu nanoparticle was synthesized as reported previously[3] and its stabilities were investigated in the presence of hydrogen peroxide, hydrogen sulfide and nitric acid. UV-vis characterization was utilized to monitor the plasmonic properties and morphological changes under different conditions. Figure S6 shows the temporal changes of the AgCu nanoparticles solution after adding 220 mM H_2O_2 (a), 0.15 mM NaHS (b) and 75 mM HNO_3 (c). The absorption peak of AgCu NPs decreased quickly within 20 minutes. Figure S6 (d-f) shows the digital photos of AgCu NPs solution after the addition of different concentrations of H_2O_2, NaHS and HNO_3 for different incubation times.

Cytotoxicity test. Measurement of cell viability was evaluated by the reduction of MTS, 3-(4，5-dimethylthiazol-2-yl)-5(3-carboxymethoxyphenyl)-2-(4-sulfopheny)-2H-tetrazolium to formazan crystals by mitochondrial dehydrogenases. A sample of 1×10^3 MCF-7 cells in 50 μL of washing buffer was seeded into each test well on a 96-well plate. After overnight culture, ACGs (0-220 μg/mL) in 50 μL of washing buffer was added to the respective test well. Then the cells were incubated at 37 ℃ in a 5% CO_2 atmosphere for 4 hours. Then the supernatant was removed and 200 μLof fresh cell culture medium was added. After 48 h of incubation at 37℃, a standard MTS assay followed. The absorbance value at 490 nm was determined by a Synergy 2 Multi-Mode Microplate Reader (Bio-Tek, Winooski, VT). The experiments were performed at least 3 times (Figure S7).

Raman detection and imaging with ACG. R6G dye was dissolved in water with a high concentration and further diluted to concentrations on demand. For each Raman spectrum, more than five measurements were performed in a Renishaw's InVia Raman system under a 633 nm excitation laser. For Raman imaging, all human breast cancer cells (MCF-7) were incubated with ACG solutions for 2 h at 37 °C. The final ACG concentration in these incubation solutions was 110 μg/mL. After washing with Dulbecco`s phosphate buffered saline (DPBS, Gibco) three times, cells were imaged under the Raman confocal microscope with a 633 nm laser. Figure S8 showed the global imaging of MCF-7cells treated with ACGs, taking only 10 seconds. The Raman signal was mainly distributed in cellular cytoplasm.

Targeted Raman cell imaging with aptamer functionalized ACG. Epithelial cell adhesion molecule (EpCAM) is overexpressed in most solid cancers. Aptamers are developed and can specifically recognize a number of live human cancer cells derived from breast, colorectal, and gastric cancers that express EpCAM but not bind to EpCAM-negative cells.[4] Such aptamer was utilized to functionalize the ACG for targeted cell and tissue imaging. The aptamer sequences (5'-CAC TAC AGA GGT TGC GTC TGT CCC ACG TTG TCA TGG GGG GTT GGC CTG AAA AAA AAA-3') were purchased from Shanghai

Biotech (China). The aptamer could be modified on the surface of ACGs by π-π stacking.[5] The efficiency of adsorbing aptamers on ACGs was also clearly demonstrated by the fluorescence spectra of 50 nM FAM-aptamer (5'-CAC TAC AGA GGT TGC GTC TGT CCC ACG TTG TCA TGG GGG GTT GGC CTG AAA AAA AAA-FAM-3') mixed with various concentrations of ACGs in 20 mM Tris-HCl buffer (pH 7.0) for 30 min (Figure S9). ACGs were able to quench FAM fluorescence through the fluorescence resonance energy transfer (FRET) process once the FAM-aptamer adsorbed on the surface.[5] Human breast cancer cells (MCF-7) and embryonic kidney cells (HEK-293) were incubated with aptamer-ACG solutions for 0.5 h at 4 °C. The final ACG concentration in these incubation solutions was 110 μg/mL. After washing with Dulbecco`s phosphate buffered saline (DPBS, Gibco) three times, cells were imaged under the Raman confocal microscope with a 633 nm laser (Figure S10). Strong Raman signals of ACGs were showed on the membrane of MCF-7 cell but not EpCAM-negative HEK-293 cell. The result further confirmed that the aptamer-ACG could selectively differentiate EpCAM-positive cells from the negative cells, which was significant for the biomedical applications.

Targeted Raman tissue imaging with aptamer functionalized ACG. The cancerous breast and normal liver tissue slices were prepared from rat frozen slices. A side of the tissue was cut flat using a vibrating-blade microtome. The slices were cultured with aptamer-ACGs (1 mg/mL) at room temperature for 40 minutes and then washed with DPBS three times for imaging. Tissues were imaged under the Raman confocal microscope with a 633 nm laser (Figure S11). Stronger signals of ACGs were detected in the cancerous tissue than the normal tissue. The result further confirmed that the aptamer-ACG can selectively differentiate cancerous from the normal tissues.

ACG SERS detection stability characterization. To demonstrate the superior stability of ACGs in the applications, we devised a SERS-based method to detect R6G molecules in the present of NaHS. Figure S12 shows the SERS spectra of R6G (1μM) enhanced with AgNPs (a) and ACGs (b) after adding 100 mM NaHS solution. The Raman signals of R6G with AgNPs were rapidly damped within 10 minutes, while that with ACGs showed no obvious changes. The ACGs indicated superior signal enhancement compared to AgNPs.

Representative SERS spectra of MCF-7 cells. Representative SERS spectra of MCF-7 cells were taken at four locations on the cell surface in the Raman images (Figure S13, S14). D, G, alkyne and the peaks from the cell components could be observed in the cell Raman images.

2. Supplementary Figures

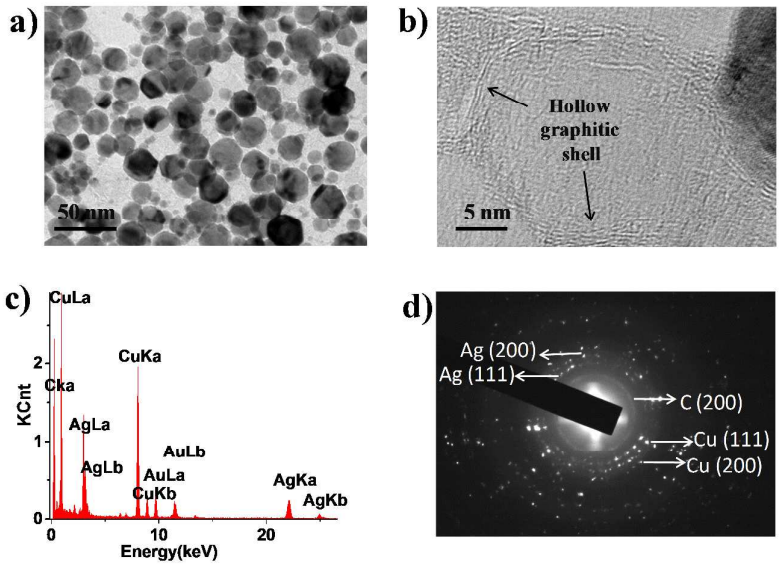

Figure S1. (a) TEM images of ACGs. (b) TEM images of the hollow graphitic shell. (c) Energy dispersive spectrometry (EDS) of ACGs. (d) selected area electron diffraction (SAED) of ACGs.

Table S1. The Ag/Cu ratio in ACGs determined by ICP-MS.

Name	Ag/Cu mass ratio	Ag/Cu molar ratio
ACG-1	2:3	2:5
ACG-2	1:2	2:7

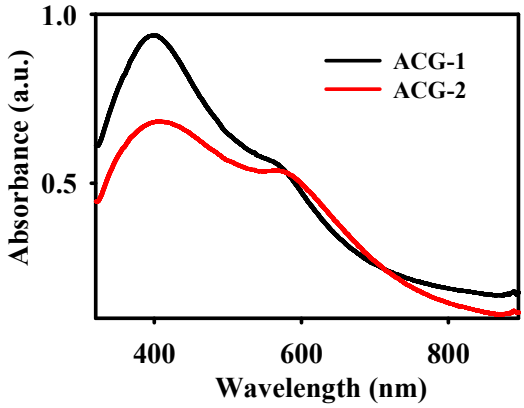

Figure S2. Uv-vis spectra of ACGs with two different Ag/Cu ratios.

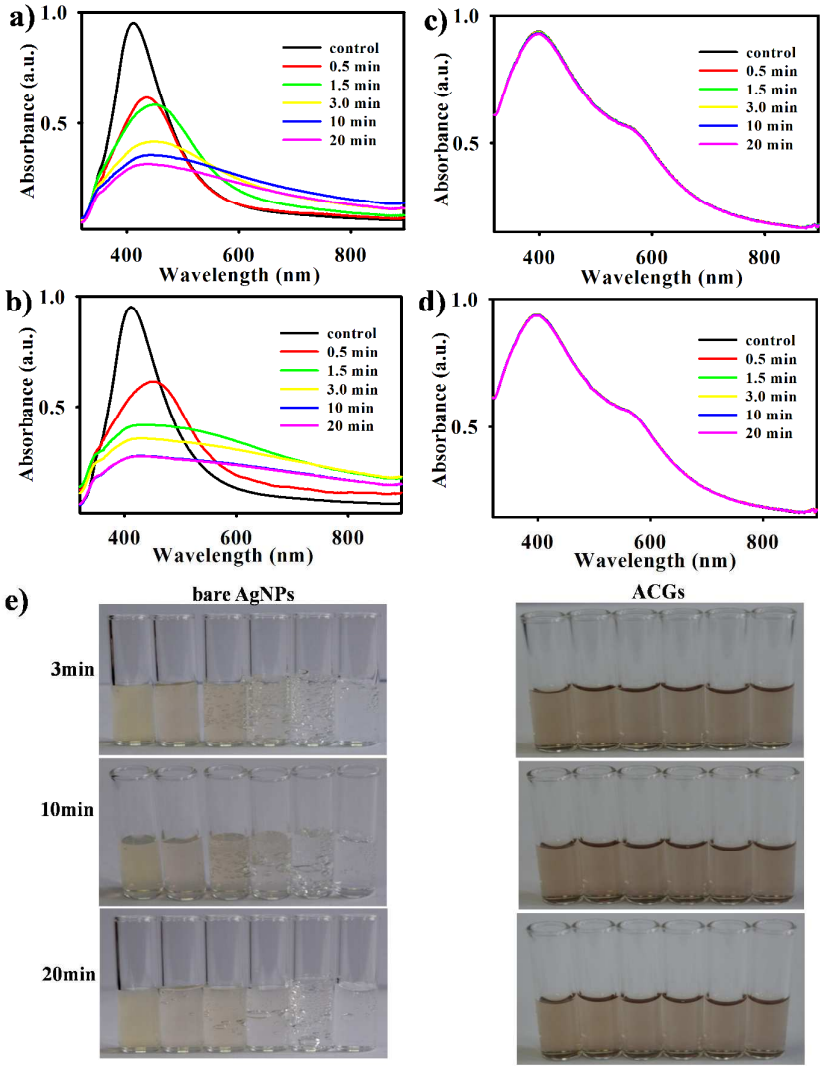

Figure S3. UV-vis spectra of bare AgNPs (a, b) and ACGs (c, d) after adding 10 and 55 mM H_2O_2 aqueous solution after different times, respectively. (e) Digital photos of bare AgNPs and ACGs suspensions after adding different concentrations of H_2O_2 (from left to right: 0, 0.10, 0.55, 0.20, 2.2, 5.5 M) aqueous solution for various times. Left: bare AgNPs; right: ACGs.

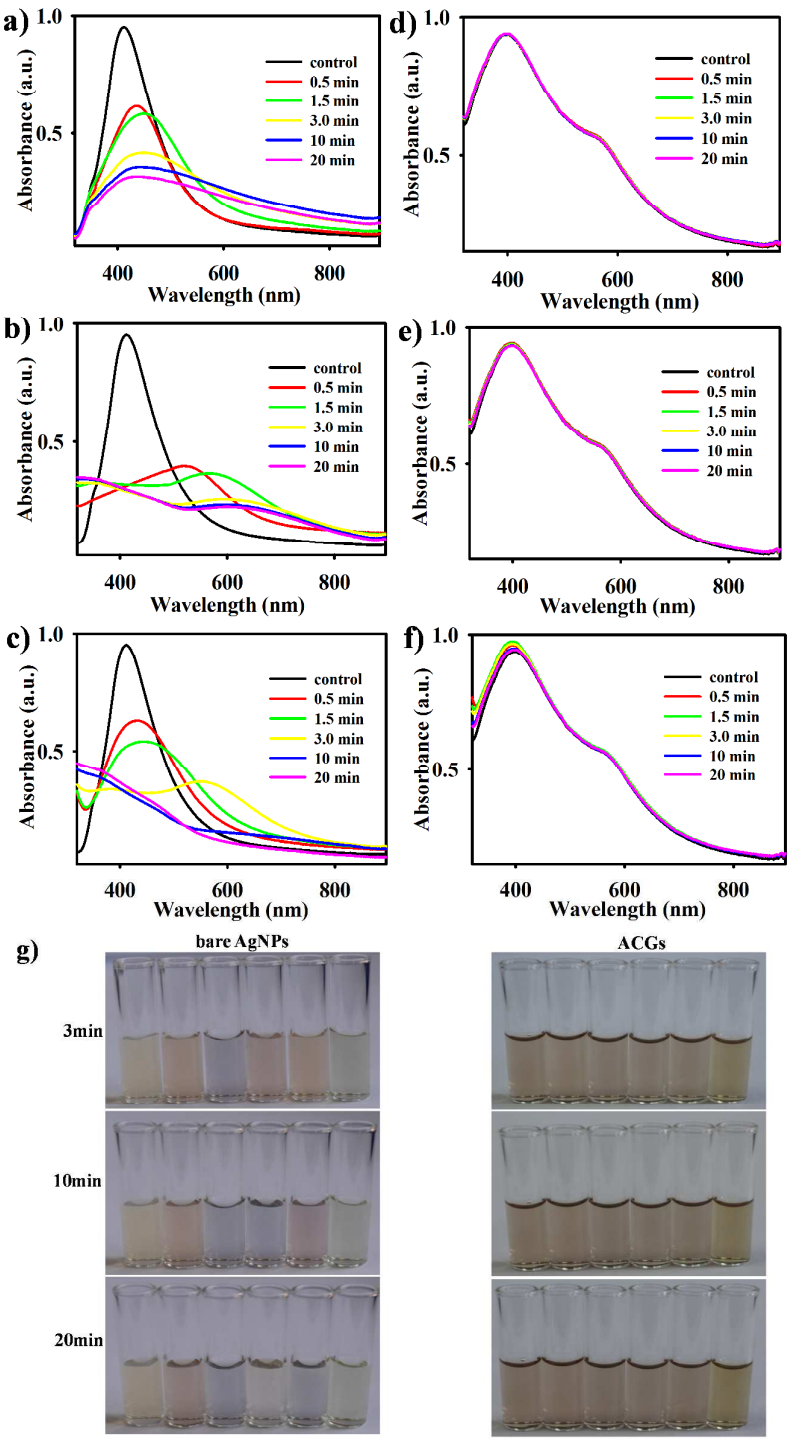

Figure S4. UV-vis spectra of bare AgNPs (a-c) and ACGs (d-f) mixed in 0.15, 0.35, and 1.5 mM NaHS aqueous solution for different times, respectively. (g) Digital photos of bare AgNPs and ACGs suspensions mixed with different concentrations of NaHS (from left to right: 0, 0.15, 0.35, 1.5, 7.5, and 75 mM) aqueous solution for various times. Left: bare AgNPs; right: ACGs.

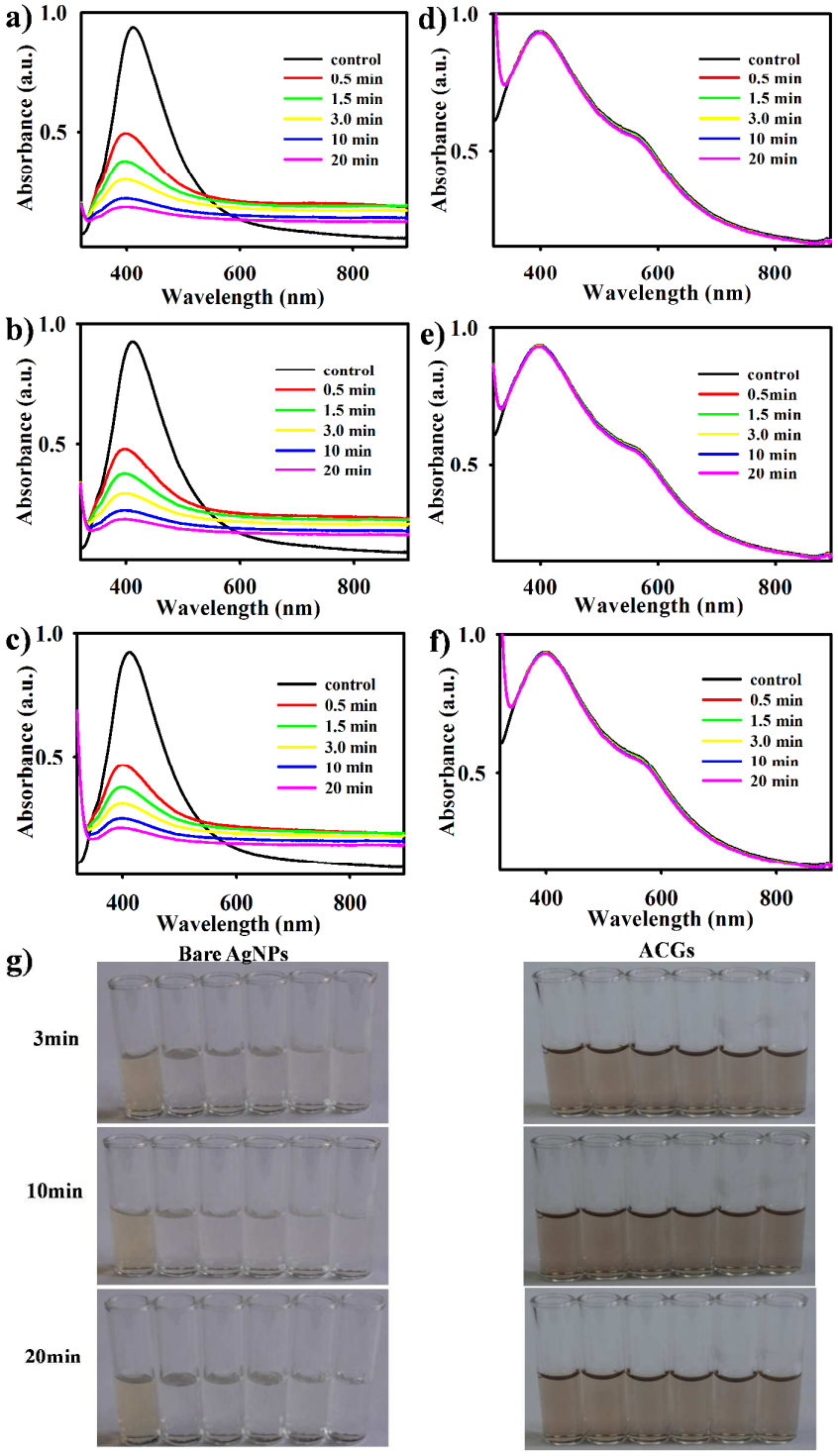

Figure S5. UV-vis spectra of bare AgNPs (a-c) and ACGs (d-f) mixed in 75, 150, and 370 mM HNO_3 aqueous solution for various times, respectively. (g) Digital photos of bare AgNPs and ACGs suspensions mixed with different concentrations of HNO_3 (from left to right: 0, 0.075, 0.15, 0.37, 1.9, and 3.7 M) aqueous solution for various times. Left: bare AgNPs; right: ACGs.

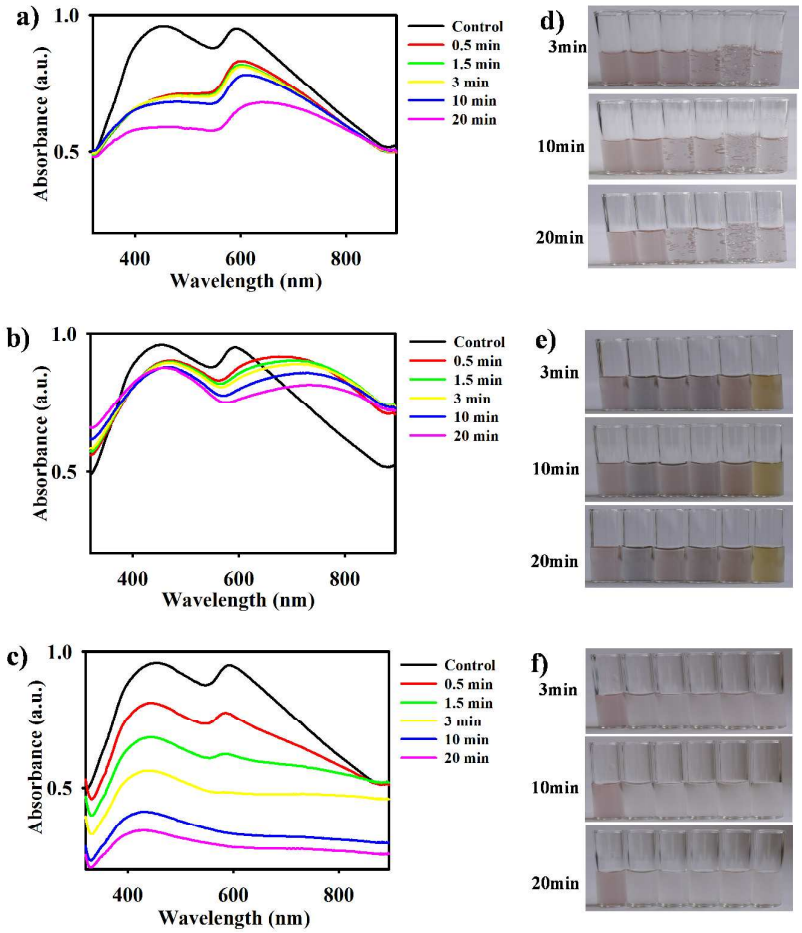

Figure S6. UV-vis spectra of bare AgCu NPs mixed in 220 mM H_2O_2 (a), 0.15 mM NaHS (b) and 75 mM HNO_3 (c) aqueous solution for different times, respectively. Digital photos of AgCu NPs suspensions mixed with different concentrations of H_2O_2 (d; from left to right: 0, 0.10, 0.55, 0.20, 2.2, 5.5 M), NaHS (e; from left to right: 0, 0.15, 0.35, 1.5, 7.5, and 75 mM) and HNO_3 (f; from left to right: 0, 0.075, 0.15, 0.37, 1.9, and 3.7 M) aqueous solution for various times.

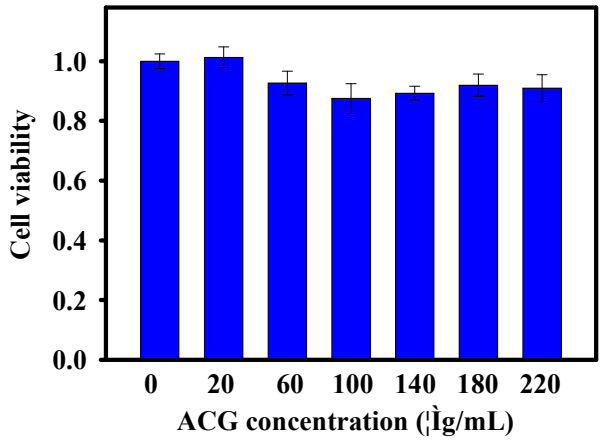

Figure S7. Cytotoxicity assay of MCF-7 cells treated with different concentration of ACGs.

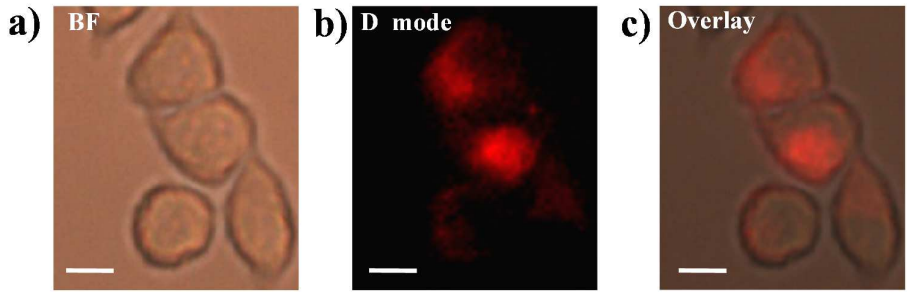

Figure S8. Global imaging of MCF-7 cells treated with ACGs under 10 s integration time in whole image. (a) Bright field image. (b) Raman image with D mode. c) The overlay of (a) and (b). BF: bright field, scale bar: 10 μm.

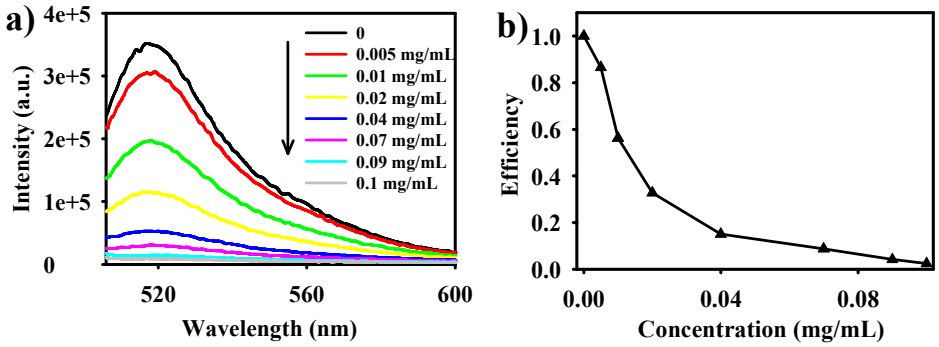

Figure S9. Quenching efficiency of the ACGs. (a) Fluorescence spectra of 50 nM FAM-aptamer mixed with various concentrations of ACGs in 20 mM Tris-HCl buffer (pH 7.0) for 30 min. (b) Quenching efficiency vs. concentration of ACGs.

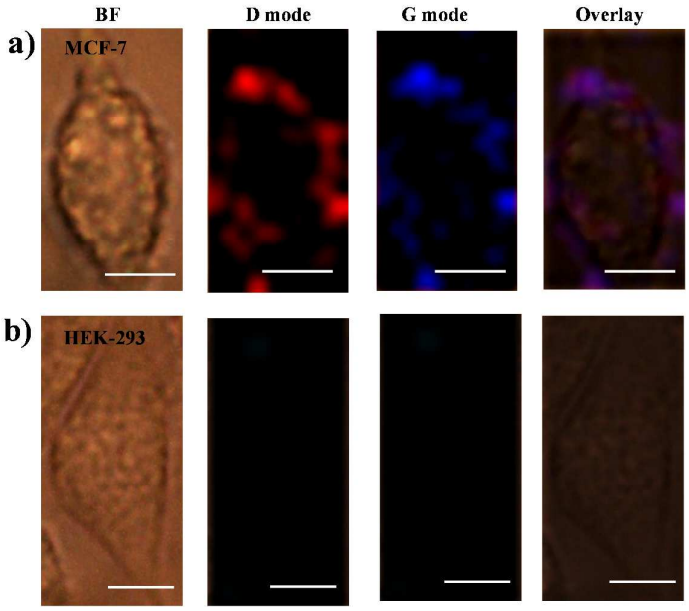

Figure S10. (a) Targeted Raman images of MCF-7 (a) and HEK-293 (b) cells treated with aptamer-ACGs at 4 °C for 30 minutes using 0.2 second integration time per pixel. BF: bright field; scale bar: 10 μm.

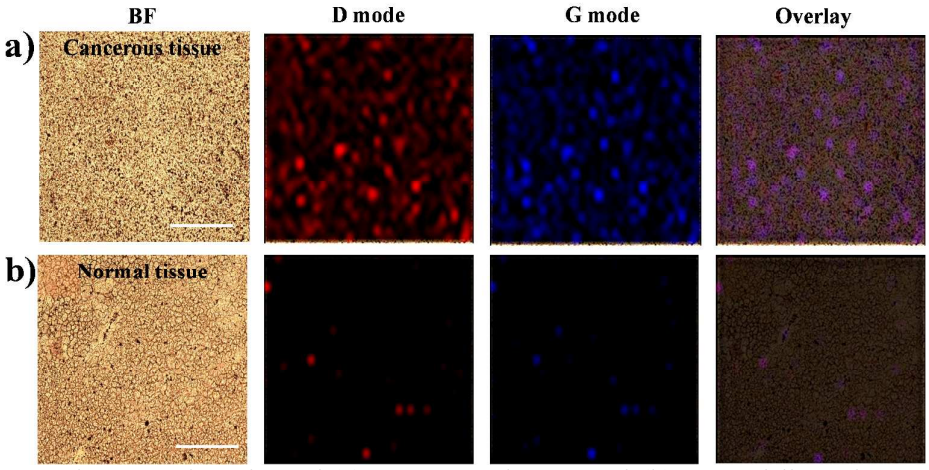

Figure S11. Targeted Raman imaging of (a) cancerous breast and (b) normal liver tissues of rat treated with aptamer-ACGs at room temperature for 40 minutes using 0.1 second integration time per pixel. BF: bright field; scale bar: 200 μm.

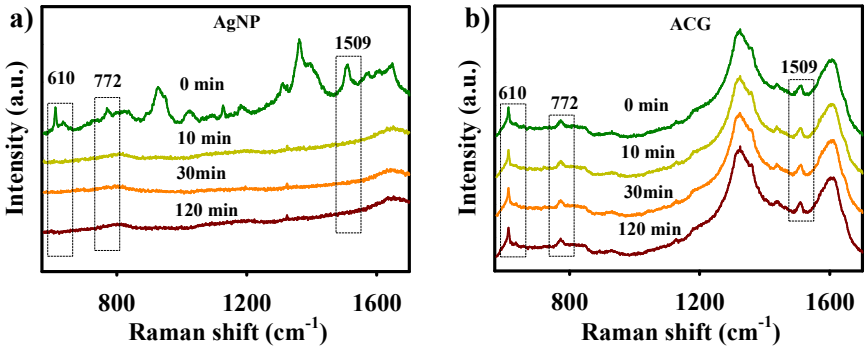

Figure S12. SERS spectra of R6G (1μM) with AgNP (a) and ACG (b) after adding 100 mM NaHS.

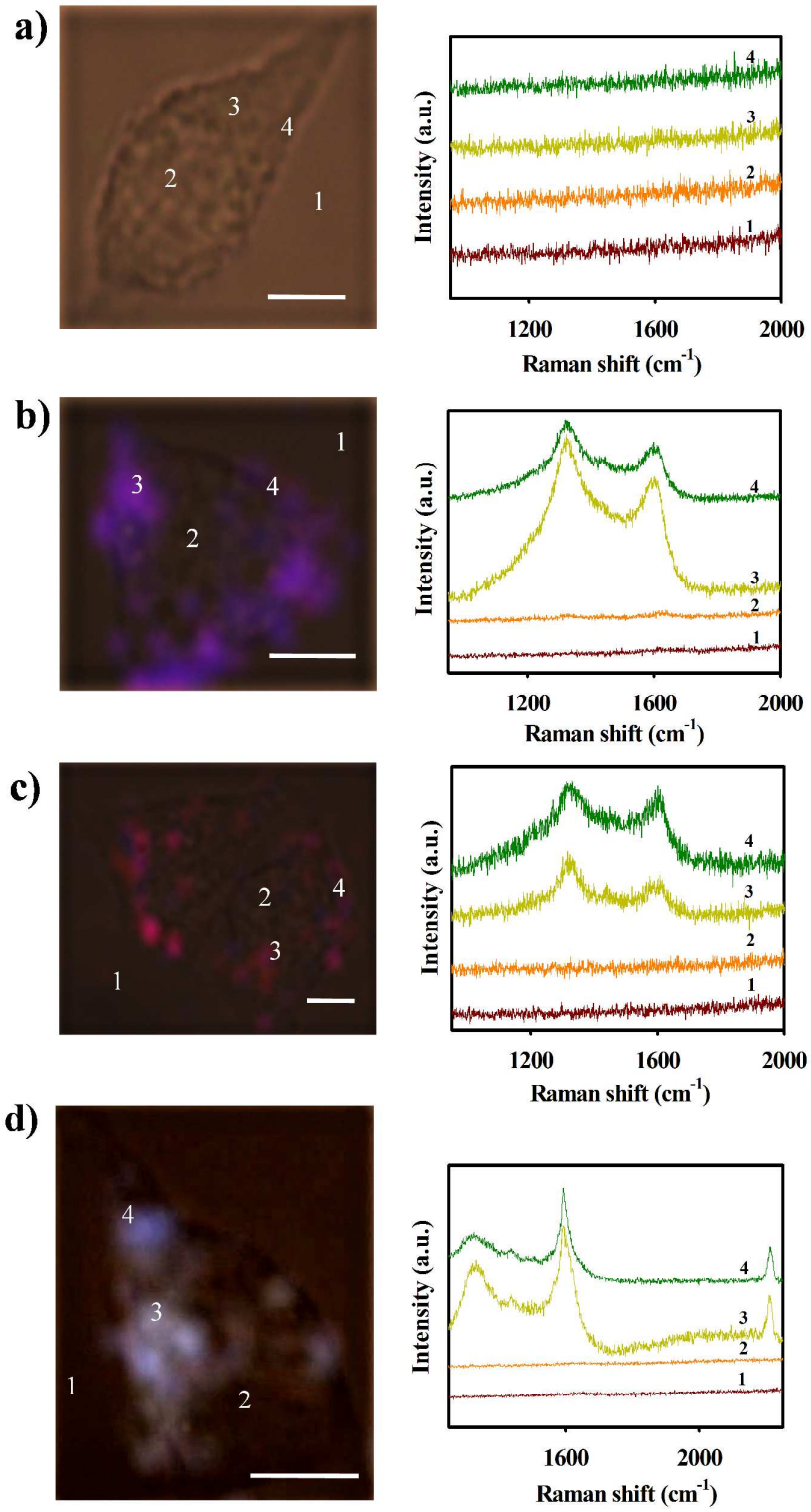

Figure S13. Representative SERS spectra of MCF-7 cells, which were taken at four locations as indicated in the left image. Raman images of MCF-7 cells treated without (a) and with ACGs (b) using 1 second integration time per pixel. (c) Rapid Raman image of MCF-7 cells treated with ACGs using 0.1 second

integration time per pixel. (d) Raman image of MCF-7 cells treated with alkyne-PEG-modified ACGs using 1 second integration time per pixel. scale bar: 10 μm.

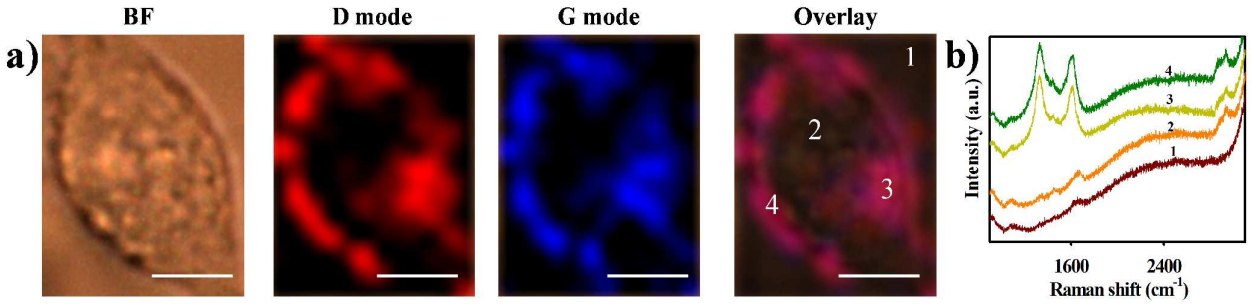

Figure S14. (a) Raman image of MCF-7 cells treated with ACGs using 1 second integration time per pixel. (b) Representative SERS spectra of MCF-7 cells, which were taken at four locations as indicated in the left image using 10 second integration time. BF: bright field; scale bar: 10 μm.

References:

1. Elie, C. -R.; Hébert, A.; Charbonneau, M.; Haiunb, A.; Schmitzer, A. R. *Org. Biomol. Chem.* **2013**, *11*, 923.
2. Almiento, G. M.; Balducci, D.; Bottoni, A.; Calvaresi, M.; Porzi, G. *Tetrahedron: Asymmetry* **2007**, *18*, 2695.
3. Huang, M.; Yang,X.; Zhao, J.; Wang, Q. *Res. Chem. Intermed* **2014,** *40*, 1957.
4. Song, Y.; Zhu, Z.; An, Y.; Zhang, W.; Zhang, H.; Liu, D.; Yu, C.; Duan, W.; Yang, C. J. *Anal. Chem.* **2013**, *85*, 4141.
5. Song, Z. L.; Zhao, X. H.; Liu, W. N.; Ding, D.; Bian, X.; Liang, H.; Zhang, X. B.; Chen, Z.; Tan, W. *Small* **2013**, 9, 951.